

Resonant electronic Raman scattering near a quantum critical point

A. M. Shvaika^{a,*} O. Vorobyov^a J. K. Freericks^b T. P. Devereaux^c

^a*Institute for Condensed Matter Physics, Lviv, Ukraine*

^b*Department of Physics, Georgetown University, Washington, DC, USA*

^c*Department of Physics, University of Waterloo, Ontario, Canada*

Abstract

We calculate the resonant electronic Raman scattering for the Falicov-Kimball model near the Mott transition on a hypercubic lattice. The solution is exact, and employs dynamical mean field theory.

Key words: Resonant Raman scattering, Falicov-Kimball model

The Falicov-Kimball model [1] has two kinds of particles: conduction electrons, which are mobile and localized electrons which are immobile. The Hamiltonian is (at half filling)

$$\mathcal{H} = -\frac{t^*}{2\sqrt{d}} \sum_{\langle ij \rangle} (c_i^\dagger c_j + c_j^\dagger c_i) + U \sum_i \left(c_i^\dagger c_i - \frac{1}{2} \right) \left(f_i^\dagger f_i - \frac{1}{2} \right), \quad (1)$$

where c_i^\dagger (c_i) creates (destroys) a conduction electron at site i , f_i^\dagger (f_i) creates (destroys) a localized electron at site i , U is the on-site Coulomb interaction between the electrons, and t^* is the hopping integral [2] (which we use as our energy unit). The symbol d is the spatial dimension, and $\langle ij \rangle$ denotes a sum over all nearest neighbor pairs (we work on a hypercubic lattice). The model is exactly solvable with dynamical mean field theory [3] when $d \rightarrow \infty$ (see [4] for a review).

The formalism for calculating the Raman response was originally developed by Shastry and Shraiman [5]. The expression for the Raman response is

$$R(\Omega) = 2\pi \sum_{i,f} \exp(-\beta \varepsilon_i) \delta(\varepsilon_f - \varepsilon_i - \Omega) \times \left| \frac{\hbar c^2}{V \sqrt{\omega_i \omega_o}} e_\alpha^i e_\beta^o \langle f | \hat{M}^{\alpha\beta} | i \rangle \right|^2 / \mathcal{Z} \quad (2)$$

for the scattering of electrons by optical photons (the repeated indices α and β are summed over). Here $\mathbf{e}^{i(o)}$ denotes the polarization vector of the incident and outgoing photon, $\varepsilon_{i(f)}$ refer to the eigenstates describing the “electronic matter”, and \mathcal{Z} is the partition function. The coupling of the photon to the electronic system is treated with the linear coupling of the vector potential to the current operator $\mathbf{j}_\alpha = \sum_{\mathbf{k}} \partial \varepsilon(\mathbf{k}) / \partial \mathbf{k}_\alpha \mathbf{c}_\mathbf{k}^\dagger \mathbf{c}_\mathbf{k}$, and the quadratic coupling of the vector potential to the stress-tensor operator $\gamma_{\alpha\beta} = \sum_{\mathbf{k}} \partial^2 \varepsilon(\mathbf{k}) / \partial \mathbf{k}_\alpha \partial \mathbf{k}_\beta \mathbf{c}_\mathbf{k}^\dagger \mathbf{c}_\mathbf{k}$, with $\varepsilon(\mathbf{k})$ the bandstructure and $c_\mathbf{k}$ the destruction operator for an electron with momentum \mathbf{k} . The scattering operator then becomes

$$\begin{aligned} \langle f | \hat{M}^{\alpha\beta} | i \rangle &= \langle f | \gamma_{\alpha,\beta} | i \rangle \\ &+ \sum_l \left(\frac{\langle f | j_\beta | l \rangle \langle l | j_\alpha | i \rangle}{\varepsilon_l - \varepsilon_i - \omega_i} \right. \\ &\left. + \frac{\langle f | j_\alpha | l \rangle \langle l | j_\beta | i \rangle}{\varepsilon_l - \varepsilon_i + \omega_o} \right), \end{aligned} \quad (3)$$

with the sum l over intermediate states.

We have evaluated these expressions for the Stokes Raman response, with an incident photon frequency

* Corresponding Author: Institute for Condensed Matter Physics of the National Academy of Sciences of Ukraine, 1 Svientsitskii Street, 79011 Lviv, Ukraine, Phone: +380-322-761054, Fax: +380-322-761158, Email: ashv@icmp.lviv.ua

ω_i , an outgoing photon frequency ω_o , and a transferred photon frequency $\Omega = \omega_i - \omega_o$. The procedure is complicated, and involves first computing the response functions on the imaginary time axis, then Fourier transforming to imaginary frequencies, and finally performing an analytic continuation to the real axis [6]. Our calculations include effects from nonresonant diagrams, from resonant diagrams, and from so-called mixed diagrams. We analyze three different symmetries of the incident and outgoing light: A_{1g} with both incident and outgoing polarizers aligned along the diagonal $\mathbf{e}^i = \mathbf{e}^o = (1, 1, \dots)$, B_{1g} with the incident light polarized along one diagonal $\mathbf{e}^i = (1, 1, \dots)$, and the outgoing light along another diagonal $\mathbf{e}^o = (1, -1, 1, -1, \dots)$, and B_{2g} with the incident light polarized along $\mathbf{e}^i = (1, 0, 1, 0, 1, 0, \dots)$ and the outgoing light polarized along $\mathbf{e}^o = (0, 1, 0, 1, 0, 1, \dots)$. The A_{1g} response has contributions from all types of processes, the B_{1g} response is nonresonant or resonant, and the B_{2g} response is purely resonant.

The Falicov-Kimball model on a hypercubic lattice has a Mott transition at half filling when $U = \sqrt{2}$. The transition is to a pseudogap-like phase, because the infinite tails of the noninteracting density of states (DOS) (which is a Gaussian) do not allow the system to have a true gap of finite width. Instead the DOS is equal to zero only at the chemical potential, and there is exponentially small DOS within a “gap region”. We examine the system just on the insulating side of the Mott transition at $U = 1.5$.

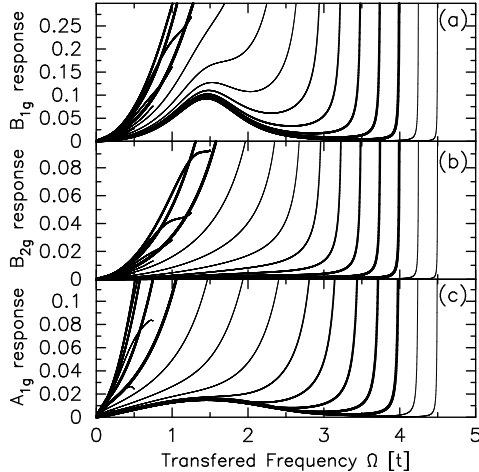


Fig. 1. The (Stokes) resonant Raman response for three different symmetries as a function of Ω (at $T = 0.05$ and $U = 1.5$; just on the insulating side of the Mott transition). The curves are for different values of the incident photon frequency.

Our results for the Raman response as a function of the transferred frequency Ω appear in Fig. 1. Note how there are strong resonant effects, including the sharp

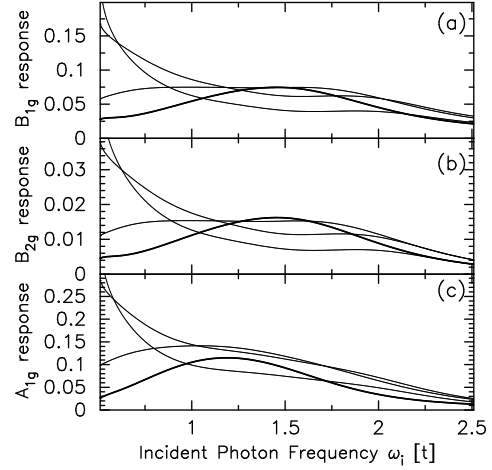


Fig. 2. Resonant profile for $\Omega = 0.5$ and various $\omega_i > 0.5$. The curves correspond to $T = 1, 0.5, 0.2$, and 0.05 in order of thinnest to thickest.

peak of the triple resonance ($\Omega = \omega_i$). Note further that the full response is not just an enhancement of the nonresonant features (which are apparent when the incident photon frequency becomes large), but that the shape of the response can change dramatically due to resonant effects. This is most apparent when the incident photon energy is close to U . In Fig. 2, we plot the resonant profile at fixed $\Omega = 0.5$ as a function of the incident photon frequency ω_i . Note how the low energy features change their resonant behavior from being centered around $\omega_i \approx 0.5 = \Omega$ (dominated by triple-resonance effects) at high temperature to being centered around $\omega_i \approx U$ at lower temperatures. This resonance of a low-energy feature, due to a higher-energy photon energy has been often seen in Raman scattering in strongly-correlated materials.

Acknowledgments: We acknowledge support from the CRDF (UP2-2436-LV-02), from the NSF (DMR-0210717) (J.K.F.) and from NSERC, PREA, and the Alexander von Humboldt foundation (T.P.D.).

References

- [1] L. M. Falicov and J. C. Kimball, Phys. Rev. Lett. **22** (1969) 997.
- [2] W. Metzner and D. Vollhardt, Phys. Rev. Lett. **62** (1989) 324.
- [3] U. Brandt and C. Mielsch, Z. Phys. B—Condens. Mat. **75** (1989) 365; **79** (1990) 295; **82**, (1991) 37.
- [4] J. K. Freericks and V. Zlatić, Rev. Mod. Phys. **75** (2003) 1333.
- [5] B. S. Shastry and B. I. Shraiman, Phys. Rev. Lett. **65** (1990) 1068; Int. J. Mod. Phys. B **5**, (1991) 365.

- [6] A. M. Shvaika, O. Vorobyov, J. K. Freericks, and T. P. Devereaux, unpublished.